0888-8809/08/$15.00/0
Printed in U.S.A.

Molecular Endocrinology 22(6):1370–1381

doi: 10.1210/me.2007-0363

Semaphorin 3B Is a 1,25-Dihydroxyvitamin D_3-Induced Gene in Osteoblasts that Promotes Osteoclastogenesis and Induces Osteopenia in Mice

Amelia L. M. Sutton,* Xiaoxue Zhang,* Diane R. Dowd, Yogendra P. Kharode, Barry S. Komm, and Paul N. MacDonald

Department of Pharmacology (A.L.M.S., X.Z., D.R.D., P.N.M.), Case Western Reserve University, Cleveland Ohio 44106; and Women's Heath Research Institute (Y.P.K., B.S.K.), Wyeth Research, Collegeville, Pennsylvania 19426

The vitamin D endocrine system is important for skeletal homeostasis. 1,25-Dihydroxyvitamin D_3 [1,25$(OH)_2D_3$] impacts bone indirectly by promoting intestinal absorption of calcium and phosphate and directly by acting on osteoblasts and osteoclasts. Despite the direct actions of 1,25$(OH)_2D_3$ in bone, relatively little is known of the mechanisms or target genes that are regulated by 1,25$(OH)_2D_3$ in skeletal cells. Here, we identify semaphorin 3B (SEMA3B) as a 1,25$(OH)_2D_3$-stimulated gene in osteoblastic cells. Northern analysis revealed strong induction of SEMA3B mRNA by 1,25$(OH)_2D_3$ in MG-63, ST-2, MC3T3, and primary osteoblastic cells. Moreover, differentiation of these osteogenic cells enhanced SEMA3B gene expression. Biological effects of SEMA3B in the skeletal system have not been reported. Here, we show that osteoblast-derived SEMA3B alters global skeletal homeostasis in intact animals and osteoblast function in cell culture. Osteoblast-targeted expression of SEMA3B in mice resulted in reduced bone mineral density and aberrant trabecular structure compared with nontransgenic littermates. Histomorphometry studies indicated that this was likely due to increased osteoclast numbers and activity. Indeed, primary osteoblasts obtained from SEMA3B transgenic mice stimulated osteoclastogenesis to a greater extent than nontransgenic osteoblasts. This study establishes that SEMA3B is a 1,25$(OH)_2D_3$-induced gene in osteoblasts and that osteoblast-derived SEMA3B impacts skeletal biology *in vitro* and *in vivo*. Collectively, these studies support a putative role for SEMA3B as an osteoblast protein that regulates bone mass and skeletal homeostasis. (*Molecular Endocrinology* 22: 1370–1381, 2008)

1,25-DIHYDROXYVITAMIN D_3 [1,25-$(OH)_2D_3$] is the bioactive metabolite of vitamin D. This hormone functions through the vitamin D receptor (VDR), a member of the nuclear hormone receptor superfamily, to regulate the transcription of target genes in a number of tissues including the intestine, bone, parathyroid gland, skin, and a variety of other systems (1, 2). The 1,25-$(OH)_2D_3$/VDR endocrine system functions in diverse biological processes, such as hair follicle cycling, mammary gland development, and immune cell function (2). One of the most profound actions of 1,25-$(OH)_2D_3$ is to protect skeletal integrity because deficiencies in either the hormone or the receptor result in undermineralized bones (3, 4).

Acting in concert with PTH, 1,25-$(OH)_2D_3$ preserves bone mineralization primarily by maintaining calcium and phosphate homeostasis. 1,25-$(OH)_2D_3$ controls serum levels of these minerals by stimulating calcium and phosphate absorption by the intestine, by increasing reabsorption of calcium and phosphate in the kidney, and by liberating calcium and phosphate from skeletal stores (3). When dietary sources of calcium are inadequate, 1,25-$(OH)_2D_3$ promotes osteoclastogenesis and bone resorption, in part, by stimulating osteoblasts to express receptor activator of nuclear factor-κB ligand (RANKL) (5), a molecule essential for osteoclast formation and function (6, 7). Under conditions of normocalcemia, the 1,25-$(OH)_2D_3$/VDR endocrine system also modulates osteoblast differentiation and mineralization (8–11). Thus, 1,25-$(OH)_2D_3$ functions both systemically to regulate serum concentrations of calcium and phosphate and locally to fine-tune the balance between bone formation and bone resorption. However, with the exception of RANKL and a few bone matrix proteins (5, 12–14), the network of target genes that mediate the effects of 1,25-$(OH)_2D_3$ on osteoblast function remain largely unknown.

First Published Online March 20, 2008

* A.L.M.S. and X.Z. contributed equally to this work.

Abbreviations: CM, Conditioned medium; μCT, microcomputed tomography; FBS, fetal bovine serum; hSEMA3B, human SEMA3B; MCSF, macrophage colony-stimulating factor; 1,25-$(OH)_2D_3$, 1,25-dihydroxyvitamin D_3; pQCT, peripheral quantitative computerized tomography; RANKL, receptor activator of nuclear factor-κB ligand; SEMA3B, semaphorin 3B; TRAP, tartrate-resistant acid phosphatase; VDR, vitamin D receptor; VDRE, vitamin D response element.

***Molecular Endocrinology* is published monthly by The Endocrine Society (http://www.endo-society.org), the foremost professional society serving the endocrine community.**

In this study, we characterize the regulation and actions of semaphorin 3B (SEMA3B), a 1,25-$(OH)_2D_3$-induced gene in osteoblasts. Semaphorins are a family of cell surface and secreted glycoproteins that were originally identified as axonal guidance proteins but subsequently have been found to regulate cell migration, cell growth, differentiation, and angiogenesis in a variety of tissues (15). SEMA3 molecules are secreted proteins that signal through neuropilin receptors (16, 17) and plexin coreceptors (18, 19). The SEMA3B gene was first identified based on its position in the chromosomal region 3p21.3, a frequent site of loss of heterozygosity in lung, kidney, ovarian, and testicular cancers (20). Reexpression of SEMA3B in either lung or ovarian cancer cells diminishes their proliferative and tumorigenic potential (21, 22), indicating that SEMA3B is also a putative tumor suppressor. SEMA3B transcripts have been detected in osteoblastic cell cultures obtained from human oral tissue explants *in vitro* (23). Moreover, neuropilin-1 expression has been detected in osteoclasts and in osteoblasts *in vitro* and *in vivo* and appears to be down-regulated as osteoblasts differentiate into more mature osteocytes (24). However, biological effects of SEMA3B in the skeletal system or in osteoblast and osteoclast function are currently unknown.

The present study characterizes SEMA3B as a novel 1,25-$(OH)_2D_3$-activated gene in multiple osteoblastic cell lines as well as in primary mouse osteoblasts. The SEMA3B transcript is also dramatically increased during osteoblastic cell differentiation, suggesting that SEMA3B may have an important role in osteoblast function. To probe the potential role(s) of osteoblast-derived SEMA3B, transgenic mice were created that express SEMA3B under the control of the osteoblast-selective 2.3-kb promoter of the mouse pro-α1(I) collagen gene. Mice that express the SEMA3B transgene exhibited decreased body weight and shorter tibiae and displayed a deficit in trabecular and cortical bone mineralization. Although osteoblast number and function appeared normal in SEMA3B transgenic mice *in vivo*, osteoclast number was dramatically increased. *In vitro* studies indicated that transgenic osteoblasts supported increased osteoclastogenesis. Thus, this study identifies osteoblast-derived SEMA3B as a novel regulator of bone mass that may function by stimulating osteoclastogenesis and osteoclast activity.

RESULTS

SEMA3B Is a 1,25-$(OH)_2D_3$-Regulated Gene in Osteoblastic Cells

Microarray analysis was used as an initial screen to identify 1,25-$(OH)_2D_3$-regulated genes in MG-63 osteoblastic cells. One highly induced transcript identified in this screen was SEMA3B, a protein involved in diverse biological processes including axon guidance, tumor suppression, and immune modulation. In this microarray screen, a 6-h treatment of MG-63 cells with 10 nM 1,25-$(OH)_2D_3$ resulted in a 10-fold induction of the SEMA3B transcript (data not shown). Northern blot analysis confirmed that 1,25-$(OH)_2D_3$ increased SEMA3B mRNA levels in a time- and dose-dependent manner (Fig. 1, A and B). This increase was evident as early as 3 h after hormone addition. Maximal induction (25-fold) was observed at 12 h (Fig. 1A). As little as 1 nM 1,25-$(OH)_2D_3$ induced SEMA3B, and transcript levels continued to increase up to 10 nM 1,25-$(OH)_2D_3$ (Fig. 1B). This increase in SEMA3B mRNA was specific for 1,25-$(OH)_2D_3$ because neither cholecalciferol, an inactive 1,25-$(OH)_2D_3$ precursor molecule, nor 24,25$(OH)_2D_3$, a vitamin D metabolite, altered SEMA3B mRNA levels (Fig. 1A and data not shown). As shown in Fig. 1C, 1,25-$(OH)_2D_3$ failed to increase SEMA3B mRNA levels when transcription was

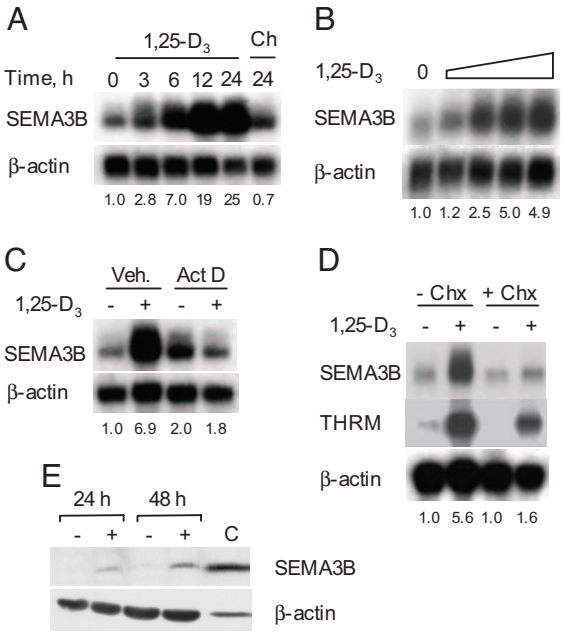

Fig. 1. 1,25-$(OH)_2D_3$ Induces SEMA3B in MG-63 Osteoblastic Cells

A, MG-63 cells were treated for the indicated times with 10^{-8} M 1,25-$(OH)_2D_3$ (1,25-D_3) or 10^{-8} M cholecalciferol (Ch). B, MG-63 cells were treated with ethanol vehicle control (0) or 0.1 to 100 nM 1,25-$(OH)_2D_3$ for 6 h. C, MG-63 cells were pretreated with methanol vehicle control (Veh.) or 1 μg/ml actinomycin D (Act D) for 1 h. Cells were then treated with ethanol control (−) or 10^{-8} M 1,25-$(OH)_2D_3$ (+) for 6 h. D, MG-63 cells were pretreated with 10 μg/ml cycloheximide (+ Chx) or ethanol control (− Chx) for 1 h. Cells were then treated with ethanol control or 10^{-8} M 1,25-$(OH)_2D_3$ (1,25-D_3) for 6 h. mRNA was isolated and analyzed by Northern blots for SEMA3B, thrombomodulin (THRM), or β-actin in *panels* A–D. *Numbers under each image* represent fold induction by 1,25-$(OH)_2D_3$. E, Western analysis of MG-63 cell extracts after 10^{-8} M 1,25-$(OH)_2D_3$ for 24 and 48 h. Lane C contains COS7 cells expressing recombinant SEMA3B as a positive control. All *panels* are representative images from one of two or more independent experiments.

blocked with actinomycin D. Furthermore, 1,25-$(OH)_2D_3$-mediated induction of SEMA3B required *de novo* synthesis of a protein factor because inhibition of protein synthesis by cycloheximide nearly abolished the response (Fig. 1D). In contrast, 1,25-$(OH)_2D_3$-induced expression of the thrombomodulin gene, a direct VDR target gene, is only marginally affected by cycloheximide treatment. Finally, Western blot analysis showed that the SEMA3B protein is also induced in MG-63 cells treated with 10^{-8} M 1,25-$(OH)_2D_3$ (Fig. 1E). Collectively, these data indicate that 1,25-$(OH)_2D_3$ increases SEMA3B mRNA and protein levels in MG-63 cells through an active transcriptional process that requires expression of one or more additional proteins.

To further establish the relevance of the vitamin D endocrine system in controlling osteoblastic expression of the SEMA3B gene, we expanded our studies to other osteoblastic model systems. ST-2 mouse bone marrow stromal cells, MC3T3 mouse fetal calvarial cells, and mouse primary calvarial osteoblasts were examined in the proliferative stage or after differentiation for 2 wk after confluence in media containing ascorbic acid and β-glycerophosphate. The proliferating or differentiating osteoblasts were treated with 1,25-$(OH)_2D_3$, and SEMA3B expression was measured by Northern blot analysis. Similar to the MG-63 cells (Fig. 1), 10 nM 1,25-$(OH)_2D_3$ also increased steady-state SEMA3B mRNA levels in a time-dependent manner in proliferating ST-2 cells, with a maximal induction of approximately 9-fold at 24 h (Fig. 2A). Treatment with 1,25-$(OH)_2D_3$ also induced SEMA3B expression in proliferating MC3T3 cells (Fig. 2C) and in primary osteoblasts (Fig. 2D). RANKL and 24-hydroxylase, established 1,25-$(OH)_2D_3$-responsive genes in osteoblastic cells, were induced as expected.

Importantly, we also observed increases in SEMA3B gene expression as these three model systems differentiated into more mature osteoblasts capable of synthesizing and secreting mineralized matrix. Differentiating ST-2 cells expressed dramatically higher levels of SEMA3B compared with its proliferative counterpart (compare lanes 1 and 3 in Fig. 2B). In addition, basal SEMA3B expression was 3-fold higher in differentiating MC3T3 cells compared with proliferating MC3T3 cells (lanes 1 and 3 in Fig. 2C). As shown in Fig. 2, A–C, 1,25-$(OH)_2D_3$ stimulated the expression of 24-hydroxlase, but the fold increase in differentiating ST-2 and MC3T3 cells was lower than in proliferating cells. Similar results were obtained with SEMA3B, namely 1,25-$(OH)_2D_3$ stimulated its expression in both proliferating and differentiating cells, but the stronger induction was apparent in proliferating MC3T3 and ST-2 cells. 1,25-$(OH)_2D_3$ also stimulated SEMA3B expression in proliferating primary osteoblasts (compare lanes 1 and 2 in Fig. 2D). SEMA3B transcripts also increased dramatically as primary osteoblasts differentiated into more mature osteoblasts (compare lanes 1 and 3 in Fig. 2D). In summary, these observations demonstrate that SEMA3B is a 1,25-$(OH)_2D_3$ target gene in numerous osteoblastic cell systems and that differentiating osteoblasts express higher levels of SEMA3B than do proliferating osteoblasts. These data suggest that SEMA3B is an important factor in 1,25-$(OH)_2D_3$-related bone physiology and perhaps in osteoblast differentiation and function.

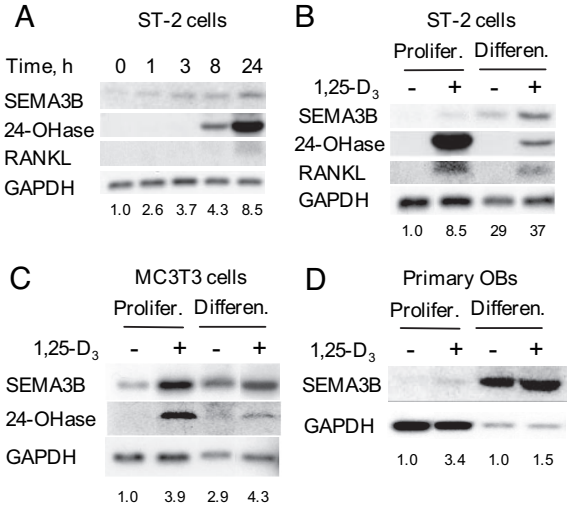

Fig. 2. SEMA3B Is Induced by 1,25-$(OH)_2D_3$ and by Differentiation of Osteoblastic Cells

A, Subconfluent ST-2 cells were treated with 10 nM 1,25-$(OH)_2D_3$ for the indicated times; B–D, subconfluent (Prolifer.) ST-2 cells (B), MC3T3 cells (C), or primary osteoblasts (D) were prepared in growth media or confluent cells were differentiated by supplementing the media with 50 μg/ml ascorbic acid and 5 mM β-glycerophosphate for 14 d (Differen.). Proliferating or differentiating cells were treated with ethanol control or 10 nM 1,25-$(OH)_2D_3$ (1,25-D_3) for 24 h. Total cellular RNA was isolated, and SEMA3B, 24-hydroxylase (24-OHase), RANKL, and GAPDH transcripts were determined by Northern blot analysis. *Numbers under each image* represent fold induction by 1,25-$(OH)_2D_3$.

SEMA3B Is Expressed in Osteoblasts *in Vivo*

To determine the *in vivo* expression of the murine SEMA3B gene, total RNA from various organs was isolated from mice, and SEMA3B transcripts were visualized by Northern blot analysis. As indicated in Fig. 3A, endogenous SEMA3B transcripts were detected in kidney, intestine, and bone. All of these are well established 1,25-$(OH)_2D_3$-target organs. The role of SEMA3B in kidney and intestine remain largely unexplored, but it is intriguing to speculate a potential connection between VDR and SEMA3B in these tissues as well. Although semaphorins are involved in axonal guidance and neural development, we detected comparatively low levels of expression of SEMA3B in whole brain extracts.

Having detected SEMA3B transcripts in skeletal tissue extracts and in various osteoblast cell lines, we employed immunohistochemistry using an antibody against SEMA3B to determine the cellular distribution of the SEMA3B protein in demineralized sections of

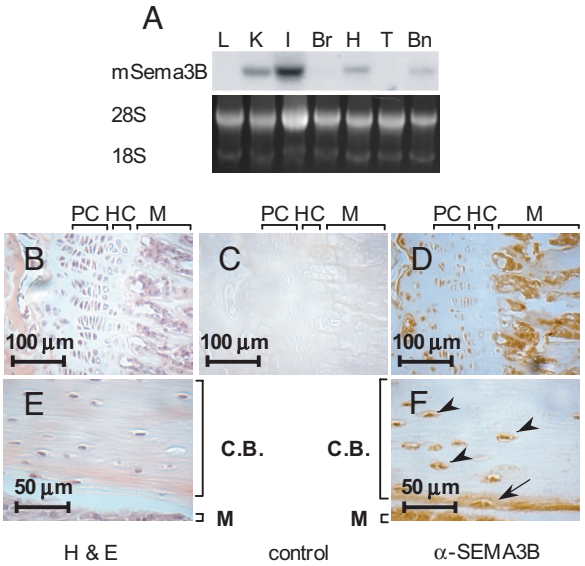

Fig. 3. SEMA3B Is Expressed in the Long Bones of Mice

A, Total RNA was extracted from indicated tissues of wild-type C57BL/6J mice, and SEMA3B expression was determined by Northern blot analysis. Ethidium bromide staining of 18S/28S rRNA was used to ensure equal loading of the RNA. Bn, Bone; Br, brain; H, heart; I, intestine; K, kidney; L, liver; T, testes. B–F, Tibiae from wild-type 8-wk-old male mice were formalin-fixed, decalcified in formic acid, embedded in paraffin, and sectioned. Serial sections were stained with hematoxylin and eosin (H & E in B and E) or immunostained in the absence (C) or presence of an affinity purified rabbit anti-SEMA3B antibody (α-SEMA3B in D and F). *Arrow* in F indicates an osteoblast on the cortical bone surface, and *arrowheads* indicate osteocytes. C.B., Cortical bone; HC, hypertrophic chondrocyte layer; M, marrow space; PC, pre-hypertrophic chondrocyte layer.

mouse tibiae. As shown in Fig. 3D, SEMA3B staining was detected in several cell types in the growth plate. SEMA3B was selectively expressed in proliferating chondrocytes within the pre-hypertrophic zone (PC in Fig. 3). Its expression was not detected in cells within the hypertrophic chondrocyte zone (HC in Fig. 3). Both osteoblasts and osteocytes expressed SEMA3B throughout the growth plate as well as in cortical bone (Fig. 3F). Additionally, staining was observed in the bone marrow (M), indicating that SEMA3B is also expressed in cells giving rise to the hematopoietic system (Fig. 3D). This was not surprising based on the known expression of other semaphorins in B cells, monocytes, hematopoietic cells, and bone marrow stromal cells (25–27).

SEMA3B-Expressing Transgenic Mice Are Smaller and Have Shorter Tibiae

SEMA3B is a secreted protein that belongs to the large semaphorin family of neurotrophic factors. Although it is known that SEMA3B is expressed in bone, the biological or cellular effects of SEMA3B on the skeleton or in osteoblasts have not been addressed previously. Therefore, we used a transgenic mouse approach to determine whether osteoblast-derived, secreted SEMA3B alters skeletal homeostasis *in vivo* and whether it impacts bone cell function *in vitro*. Similar approaches have been useful in uncovering the biological activity of other signaling proteins in the skeleton (28–30). Thus, transgenic mice were created in which human SEMA3B (hSEMA3B) expression was driven by the osteoblast-selective mouse 2.3-kb pro-α1(I) collagen promoter. Two lines of transgenic mice were established. Line 2 showed robust expression of SEMA3B in Northern blot assays (Fig. 4B), whereas line 1 showed lower expression of the transgene that was only detected using more sensitive RT-PCR approaches (Fig. 4B and data not shown).

To confirm that the hSEMA3B transgene is selectively expressed in bone of line 2 transgenic mice, a tissue distribution Northern blot analysis was performed (Fig. 4C). The hSEMA3B transgene was detected only in bone RNA from line 2 transgenic mice. A weak signal was present in intestinal RNA in both nontransgenic and transgenic littermates, suggesting cross-hybridization of the human cDNA probe with the abundant murine SEMA3B transcript in the intestine. Using a murine cDNA probe, we confirmed that the endogenous SEMA3B transcript levels were similar in tissues of line 2 transgenic mice compared with nontransgenic littermate controls (data not shown).

The low-expressing line 1 transgenic mice were comparable in size to their nontransgenic littermates (data not shown). However, male transgenic mice from line 2 were smaller compared with nontransgenic littermates, displaying a 34% reduction in body weight (Fig. 4, A and D). Female transgenic mice had a similar decrease in body weight (data not shown). Furthermore, line 2 transgenic mice exhibited a 6% reduction in tibia length compared with their nontransgenic littermates (Fig. 4E).

SEMA3B Transgenic Mice Have Reduced Bone Mineral Density and Altered Trabecular Structure

Tibiae from male transgenic mice and their nontransgenic littermates were analyzed by peripheral quantitative computerized tomography (pQCT) to determine bone mineral densities. The low-expressing line 1 transgenic mice showed no significant differences in bone density compared with their nontransgenic littermates (data not shown). Remarkably, tibiae from the higher-expressing line 2 mice displayed dramatic reductions in trabecular, cortical, and total bone mineral density (Fig. 5). The microarchitecture of the trabecular bone was also dramatically altered as determined with high-resolution microcomputed tomography (μCT) (Fig. 6A). Consistent with the pQCT analysis, μCT measurements indicated that transgenic bones had decreased trabecular bone volume (BV/TV) with an increase in the exposed surface of trabecular bone (BS/BV; Fig. 6B). Transgenic bones had significantly fewer and thinner trabeculae as com-

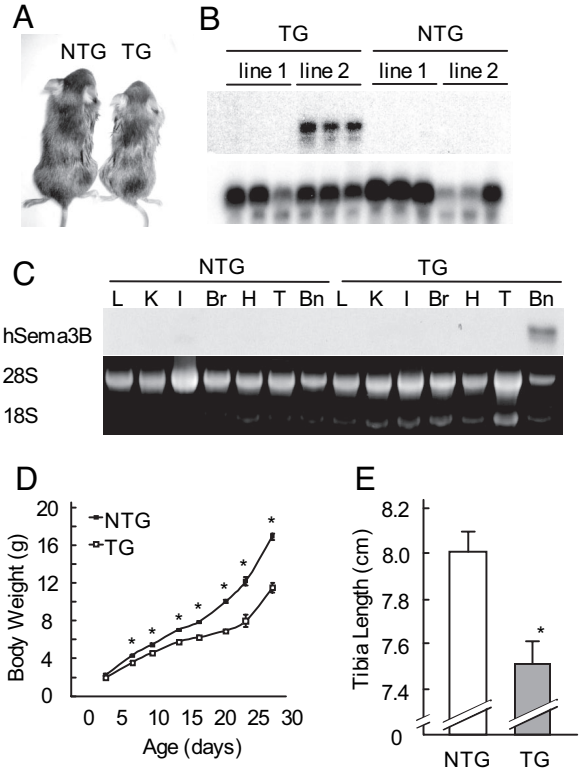

Fig. 4. Transgenic Mice with Targeted Osteoblast-Selective Expression of SEMA3B Have Reduced Body Weight and Shorter Bones

A, Photograph of 31-d-old male nontransgenic and transgenic littermates. B, The SEMA3B transgene is expressed robustly in long bones of line 2 transgenic mice. Total humerus RNA from three transgenic or three nontransgenic littermates from two independent lines of mice was analyzed by Northern blot for hSEMA3B and β-actin expression. C, Total RNA was isolated from the indicated organs of nontransgenic or line 2 transgenic mice. Transgene expression was analyzed by Northern blot using a human SEMA3B cDNA probe. Equal RNA loading was normalized by the band intensity of ethidium bromide-stained 18S/28S rRNA. Bn, Bone; Br, brain; H, heart; I, intestine; K, kidney; L, liver; T, testes. D, Growth curve of male NTG and TG mice. Data represent mean $\pm$ SEM; n $\geq$ 5 in each group. *, $P < 0.01$ by Student's *t* test. E, pQCT measurement of left tibia length; n = 8 in each group. *, $P < 0.01$ by Student's *t* test. NTG, Nontransgenic; TG, transgenic.

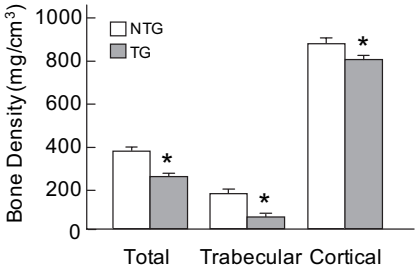

Fig. 5. SEMA3B-Expressing Transgenic Mice Have Decreased Bone Mineral Density

pQCT analysis of total, trabecular, and cortical bone density of tibiae from 31-d-old male nontransgenic (NTG) and transgenic (TG) littermates. Data represent mean $\pm$ SEM; n = 7–8 in each group. *, $P < 0.02$ by Student's *t* test.

pared with nontransgenic littermates (Fig. 6B). Furthermore, there was increased spacing between trabeculae and a dramatic reduction in the connectivity density in the trabecular network of the transgenic bones (Fig. 6B). Together these results indicate that SEMA3B transgenic animals have reduced trabecular bone and decreased bone density.

SEMA3B Transgenic Mice Have Increased Osteoclasts and Bone Resorption

To explore potential cellular mechanisms underlying the trabecular bone defect in the transgenic mice, histomorphometric analysis was performed to examine osteoblastic and osteoclastic parameters (Fig. 7). There were no alterations in osteoblast cell number in SEMA3B transgenic tibiae as compared with nontransgenic mice (Fig. 7A). Likewise, dynamic histomorphometric measurements of calcein- and tetracycline-labeled bone indicated that transgenic animals had a normal mineral apposition rate, a measurement of osteoblastic activity (Fig. 7B). In contrast, tibiae obtained from transgenic animals displayed a significant increase in the number of osteoclasts per unit bone surface area (Fig. 7C). This increase in osteoclast number was reflected in a more than 2-fold enhancement of bone resorption as measured by the percentage of bone surface undergoing erosion (Fig. 7D). In agreement with the μCT imaging studies in Fig. 6, the histomorphometry also documented statistically significant decreases in trabecular bone volume and trabecular number (data not shown). Collectively, the imaging and histomorphometry data clearly indicate that there is a reduction in bone mineral density and trabecular architecture that is not the result of impaired osteoblastic activity but rather increased osteoclastogenesis and bone resorption in SEMA3B transgenic mice.

Transgenic Osteoblasts Display Increased Differentiation and Mineralization *in Vitro*

To determine the cellular basis for the low bone density in the SEMA3B-expressing transgenic mice, we examined osteoblast differentiation and osteoblast-induced osteoclastogenesis *in vitro* using osteoblasts derived from nontransgenic and SEMA3B-expressing transgenic mice (Fig. 8). As shown in Fig. 8A, SEMA3B-expressing osteoblasts showed appropriate transgene expression in differentiated osteoblast cultures after 2 wk in culture with ascorbic acid and β-glycerophosphate. Minimal SEMA3B transgene expression was detected in proliferating osteoblast cultures obtained from either nontransgenic or transgenic mice. In contrast, significant expression was observed in differentiating osteoblasts obtained from the

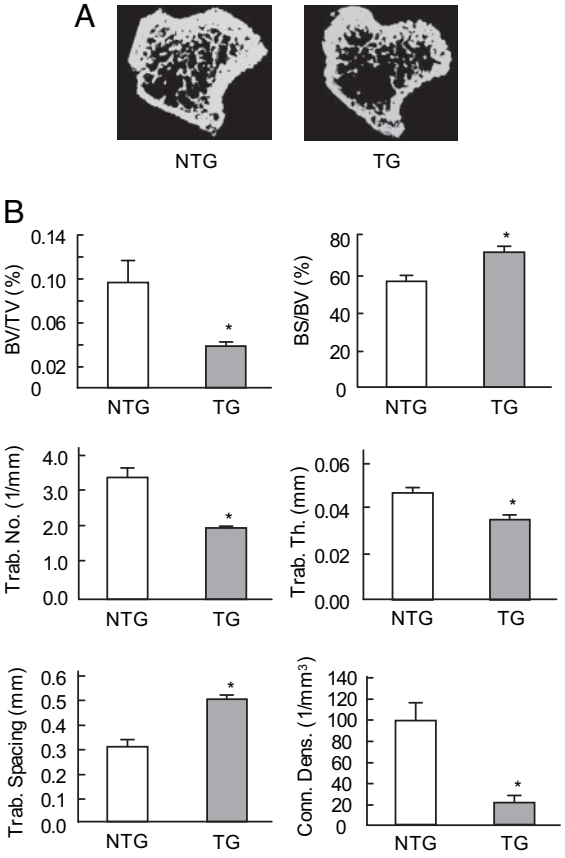

Fig. 6. Transgenic Mice Have Diminished Trabecular Bone

A, μCT cross-sectional images of representative tibiae from 31-d-old male nontransgenic (NTG) and transgenic (TG) littermates. B, Quantitative μCT shows decreased trabecular bone volume. BS/BV, bone surface expressed as a percentage of total trabecular volume; BV/TV, trabecular bone volume expressed as a percentage of total tissue volume; Conn. Dens., connectivity density of trabecular bone; Trab. No., number of trabeculae per millimeter; Trab. Spacing, trabecular spacing; Trab. Th., trabecular thickness. Data represent mean ± SEM; n = 8 in each group. *, $P < 0.01$ by Student's *t* test.

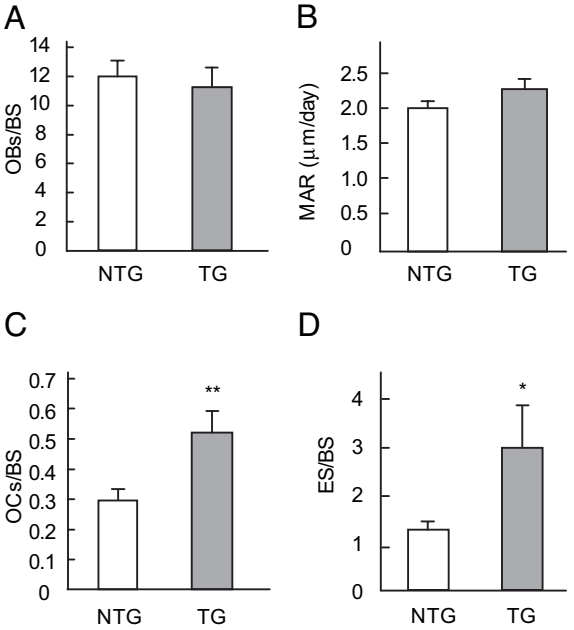

Fig. 7. Transgenic Bones Have Normal Osteoblasts but Increased Osteoclastogenesis

Histomorphometry measurements were performed on sections of tibiae from nontransgenic (NTG) and transgenic (TG) 31-d-old male mice that had been double labeled with calcein and tetracycline. A, Number of osteoblasts per millimeter of bone surface (OBs/BS); B, mineral apposition rate MAR; C, number of osteoclasts per millimeter of bone surface (OCs/BS); D, percentage of bone surface involved in resorption (ES/BS). Data represent mean ± SEM; n = 10 in each group. **, $P < 0.02$ by Student's *t* test; *, $P = 0.07$ by Student's *t* test.

SEMA3B-expressing mice but not the nontransgenic controls (Fig. 8A). Thus, appropriate expression of the transgene driven by the 2.3-kb promoter region of the mouse pro-α1(I) collagen gene was observed in this *in vitro* primary cell culture. Coincident with enhanced expression of the SEMA3B transgene, differentiating cultures from transgenic mice also expressed modestly higher levels of alkaline phosphatase, a marker of osteoblast differentiation, as compared with osteoblasts derived from nontransgenic littermates (Fig. 8B). This was particularly evident in the late-stage mineralizing osteoblast cultures. Enhanced mineralized nodule formation was also observed in transgenic osteoblast cultures (Fig. 8, C–E). It is important to note that cultures obtained from either line 2 or line 1 mice displayed enhanced alkaline phosphatase expression compared with their respective nontransgenic littermate controls. Thus, osteoblasts obtained from two independent SEMA3B-expressing transgenic lines showed modestly enhanced differentiation compared with nontransgenic control osteoblasts. These data collectively indicate that overexpression of SEMA3B does not impair, but rather may promote, osteoblastic differentiation *in vitro*.

Because histomorphometric analysis suggested that osteoclastogenesis was increased in transgenic mice, we also compared the ability of transgenic and nontransgenic osteoblasts to support *in vitro* osteoclast formation from spleen cell precursors (Fig. 9). Primary osteoblasts derived from transgenic and nontransgenic mice were differentiated for 15 d and then cocultured with wild-type osteoclast precursor cells in the presence of dexamethasone and 1,25-$(OH)_2D_3$. In the absence of 1,25-$(OH)_2D_3$, no osteoclastogenesis was observed in the coculture using transgenic or nontransgenic osteoblasts (data not shown). As shown in Fig. 9, A–C, significantly more multinucleated, tartrate-resistant acid phosphatase (TRAP)-positive, 1,25-$(OH)_2D_3$-induced cells indicative of osteoclasts formed in the cocultures with transgenic osteoblasts as compared with nontransgenic osteoblasts. These *in vitro* data support the *in vivo* obser-

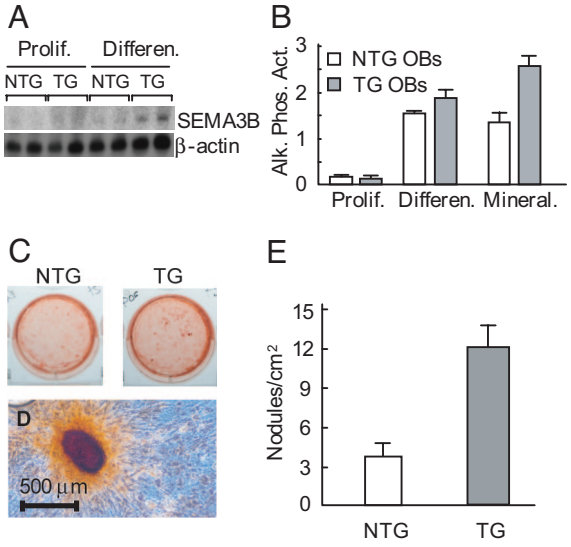

Fig. 8. *In Vitro* Analysis of Osteoblast Differentiation

A, SEMA3B transgene expression increases during osteoblast differentiation. Primary osteoblasts were isolated from the calvaria of newborn nontransgenic and transgenic mice. For differentiation, confluent osteoblasts were cultured in growth medium supplemented with 50 μg/ml ascorbic acid and 10 mM β-glycerophosphate for 15 d. Total RNA was isolated and analyzed for hSEMA3B and β-actin expression by Northern blot. B, *In vitro* differentiation of nontransgenic and transgenic osteoblasts. Primary osteoblasts from transgenic and nontransgenic animals were isolated and differentiated as in A. Alkaline phosphatase activity (Alk. Phos. Act.) was determined at the indicated stages [proliferating (Prolif.), d 6; differentiated (Differen.), d 15; and mineralization (Mineral.), d 25] by measuring conversion of *p*-nitrophenyl phosphate to *p*-nitrophenol. Activity was normalized to protein concentration. Data represent the mean of triplicate well ± SEM and are representative of three separate experiments. C and D, Primary osteoblasts from transgenic and nontransgenic animals were isolated and differentiated as in A. On d 31, the cells and mineralized nodules were stained with alizarin red S. Representative images are shown in C. A high-magnification image of one alizarin red S-positive nodule is depicted in D. Mineralized nodules were counted, and the data are presented in E. Data represent the mean of triplicate wells ± SEM and are representative of three separate experiments. NTG, Nontransgenic; TG, transgenic.

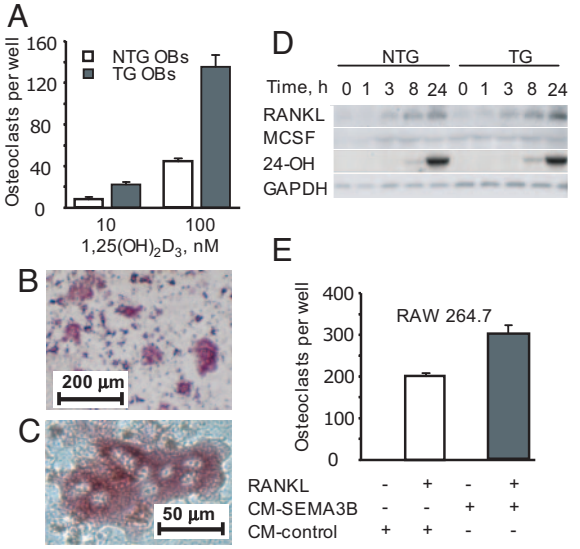

Fig. 9. SEMA3B-Stimulated Osteoclastogenesis

Confluent primary osteoblasts derived from newborn nontransgenic (NTG) or transgenic (TG) mice were cultured in medium containing 50 μg/ml ascorbic acid and 10 mM β-glycerophosphate for 15 d. Osteoclast precursors derived from the spleens of wild-type adult mice were added to the osteoblast cultures and grown for an additional 8 d in the presence of 100 nM dexamethasone and either 0, 10, or 100 nM 1,25-$(OH)_2D_3$. Multinucleated osteoclasts were visualized by staining for TRAP activity as described in *Materials and Methods*. A, Number of TRAP-positive multinucleated (at least three nuclei) cells per well. Values are the mean ± SEM of triplicate wells and are representative of four separate osteoblast and spleen cell preparations. B, Representative fields of TRAP-positive multinucleated cells from transgenic osteoblasts stimulated with 100 nM 1,25-$(OH)_2D_3$. C, high-magnification image of one TRAP-positive multinucleated cell. D, Differentiating primary osteoblasts derived from nontransgenic or transgenic mice were treated with 100 nM 1,25-$(OH)_2D_3$ for indicated time, and the expression levels of RANKL, MCSF, 24-hydroxylase (24-OHase), and GAPDH were determined by Northern blot analysis. E, SEMA3B-containing CM (CM-SEMA3B) and control medium (CM-control) from transfected COS7 cells were prepared as described in *Materials and Methods*. RAW 264.7 cells were cultured in 50% of CM in the absence or presence of 20 ng/ml RANKL for 72 h and stained for TRAP. The numbers of TRAP-positive multinucleated (at least three nuclei) cells in each well were counted. Values are the mean ± SEM, and a representative result of four independent experiments is shown in E.

vation that overexpression of SEMA3B in osteoblasts stimulates osteoclastogenesis. To investigate a potential mechanistic basis for increased osteoclastogenesis by the SEMA3B-expressing osteoblasts, we determined the level of expression of several osteoblast-derived factors that impact osteoclastogenesis, including RANKL, osteoprotegerin, macrophage colony-stimulating factor (MCSF), IL-1β, IL-6, and TNFα in the transgenic and nontransgenic primary osteoblast cultures. Overt differences in transcript levels for these factors were not apparent in the transgenic and nontransgenic osteoblasts (Fig. 9D and data not shown), suggesting that osteoblast-targeted SEMA3B does not alter RANKL expression or the expression of other key osteoclastogenic factors in primary osteoblasts. Instead, SEMA3B signaling within osteoclast progenitor cells may enhance the RANK-RANKL pathway and promote osteoclastogenesis. This possibility is supported by studies depicted in Fig. 9E using the RAW264.7 osteoclast progenitor cell line. This murine macrophage cell line responds to RANKL stimulation *in vitro* by forming TRAP-positive, multinucleated fully differentiated osteoclasts. Although recombinant SEMA3B alone had no effect, it dramatically enhanced RANKL-mediated osteoclast differentiation of the RAW264.7 progenitor cell line. Thus, these data sup-

port a positive role for SEMA3B signaling in the RANK-RANKL pathway that is required for differentiation of osteoclast precursors into mature, multinucleated, bone-resorbing cells.

DISCUSSION

The primary role of the vitamin D endocrine system is to tightly control serum concentrations of mineral ions by driving intestinal absorption of calcium and phosphate. However, when dietary sources of calcium are lacking, 1,25-$(OH)_2D_3$ stimulates bone resorption by increasing osteoclastogenesis and osteoclast activity (3). The effects of 1,25-$(OH)_2D_3$ on osteoclasts are thought to be mediated by signaling through osteoblasts. Specifically, 1,25-$(OH)_2D_3$ stimulates osteoblasts to express RANKL (5), a cytokine that is essential for osteoclastogenesis and osteoclast activity (6, 7). However, beyond increasing RANKL signaling, the precise mechanisms governing osteoblast-osteoclast communication by 1,25-$(OH)_2D_3$ are not well understood. In the present study, we show that SEMA3B is a 1,25-$(OH)_2D_3$-induced gene in osteoblastic cells and provide evidence, through targeted expression of SEMA3B in mouse osteoblasts, that osteoblast-derived SEMA3B results in reduced bone mineral density. These studies are the first to demonstrate a potential biological role for SEMA3B in skeletal homeostasis.

Our studies show that SEMA3B transcripts are strongly induced by 1,25-$(OH)_2D_3$ in a variety of osteoblastic cells. Although the precise regulatory mechanisms remain unclear, inhibitor studies indicate that this is a transcriptional response to 1,25-$(OH)_2D_3$ that requires ongoing protein synthesis (Fig. 1, C and D). Detailed promoter analysis is required to rigorously address the mechanism of regulation by 1,25-$(OH)_2D_3$. In this regard, putative vitamin D response elements (VDREs) were recently identified downstream of the transcriptional start site in the human SEMA3B gene (at positions +1907 to +2029), and chromatin immunoprecipitation studies indicated a 1,25-$(OH)_2D_3$-dependent recruitment of native VDR to this region in the SCC25 squamous carcinoma cell line (31). However, the functional relevance of this region of the human SEMA3B gene has not been addressed as yet. In our hands, this region does not serve as a high-affinity binding site for VDR-retinoid X receptor heterodimers *in vitro*, and it does not drive VDR/1,25-$(OH)_2D_3$-dependent expression of a heterologous TK promoter in a manner similar to established DR-3 VDREs from the rat osteocalcin or 24-hydroxylase genes (data not shown). This, combined with the atypical VDRE sequences identified in this region (31), suggests the potential for alternative mechanisms of regulation. Thus, our cycloheximide data suggest that the regulation of SEMA3B may be wholly mediated by another 1,25-$(OH)_2D_3$-induced transcription factor(s) or that a newly synthesized factor(s) cooperates with VDR to stimulate SEMA3B expression in osteoblastic cells, perhaps through these downstream VDR binding sites. Defining the mechanisms involved in 1,25-$(OH)_2D_3$-mediated expression of SEMA3B transcripts in osteoblasts is an important goal, particularly in light of the impact that osteoblast-driven SEMA3B expression has on overall *in vivo* skeletal homeostasis.

Most reports on semaphorins focus on the role of these signaling proteins in axon guidance and neural development. Only recently has the role of semaphorins in other important physiological and pathological systems been reported (32, 33). Studies addressing the expression or role of semaphorins in the skeleton are limited. Previous reports demonstrated that SEMA3B transcripts as well as transcripts for many other semaphorin family members, their neuropilin receptors, and plexin coreceptors are expressed in osteoblast-enriched cell populations obtained from periodontal and gingival isolates *in vitro* (23). SEMA3A and its receptors have distinct expression patterns during endochondral ossification (34, 35). SEMA3A deletion in mice leads to widespread skeletal abnormalities, including vertebral fusions, rib duplications, and a thickened sternum (34, 35). This indicates a role for SEMA3A in skeletal development and patterning. SEMA7A is another family member whose expression is regulated by osteoblast differentiation *in vitro* (36, 37). In contrast to SEMA3B, SEMA7A expression is down-regulated during the differentiation of primary osteoblasts and MC3T3 cells, implying that each type of semaphorin glycoprotein may play distinct roles in bone development and homeostasis. In support of this role, a SEMA7A polymorphism was shown to be associated with low bone mineral density and fracture risk in women (36).

The SEMA3B protein is expressed in osteoblasts, mature osteocytes, and pre-hypertrophic chondrocytes *in vivo* (Fig. 3). In contrast, SEMA3A is present in osteoblasts, osteoclasts, pre-hypertrophic, and hypertrophic chondrocytes (34, 35). SEMA3B was characteristically absent from the hypertrophic chondrocyte layer of the growth plate (Fig. 3D). Although we cannot exclude osteoclast expression of SEMA3B, strong staining for SEMA3B was not observed in multinucleated cells lining the mineralized matrix. Osteoblast and chondrocyte expression of these semaphorins suggest that secreted semaphorin signaling may be important for skeletal development and homeostasis. Importantly, the SEMA3B-expressing transgenic mouse provides important support for this possibility.

Osteoblast-directed expression of SEMA3B in mice led to a dramatic skeletal phenotype including decreased longitudinal bone growth (Fig. 4E) and undermineralized cortical and trabecular bone, most likely the result of increased osteoclast number. Consistent with these findings, *in vitro* coculture studies showed that transgenic osteoblasts stimulated increased osteoclastogenesis as compared with nontransgenic os-

teoblasts (Fig. 9, A–D). Taken together, these data suggest that the osteopenia observed in SEMA3B transgenic mice was not due to impaired osteoblast function but rather a result of increased osteoclastogenesis and osteoclast activity. These findings are analogous to transgenic mice expressing Cbfa1 (29), a transcription factor essential for osteoblast differentiation in mature osteoblasts (38, 39). Although Cbfa1-overexpressing mice display normal mineral apposition rates, they have increased osteoclastogenic parameters *in vivo* leading to low bone mass (29). Furthermore, osteoblasts derived from these animals support *in vitro* osteoclast formation to a greater extent than nontransgenic osteoblasts (29). Although the mechanisms remain unclear, this phenotype correlated with enhanced expression of RANKL in the Cbfa1 model.

In contrast to the Cbfa1 transgenic mouse, expression levels of RANKL and numerous other osteoblast-derived osteoclastogenic factors (including IL-1β, IL-6, osteoprotegerin, and MCSF) do not differ in the SEMA3B-expressing osteoblasts compared with nontransgenic controls (Fig. 9). Yet, SEMA3B-expressing osteoblasts show an increased capacity to promote osteoclastogenesis in the coculture system (Fig. 9). These data suggest that the osteoclastogenic effect of SEMA3B may be direct. Indeed, osteoclasts express neuropilin-1, one of the receptors for secreted semaphorins (24), and recent studies have shown that rac1, an effector of semaphorin signaling (40), is required for osteoclast differentiation and bone resorption (41, 42). Thus, SEMA3B may bind neuropilin-1 expressed on the surface of osteoclast precursors and signal through rac1 to directly promote osteoclastogenesis. We tested this potential mechanism in the more defined RAW246.7 cell system (Fig. 9E). Here, direct stimulation of RAW246.7 cells with conditioned medium (CM) containing recombinant SEMA3B showed no induction of osteoclast formation arguing against a direct stimulation of osteoclastogenesis via the semaphorin/neuropilin signaling system. However, recombinant SEMA3B dramatically enhanced RANKL-stimulated osteoclastogenesis of RAW246.7 cells. Cumulatively, these data support a mechanism involving SEMA3B-activated signaling cascades in osteoclast precursors impinging upon and positively affecting the RANKL pathway to promote osteoclast differentiation.

In osteoblastic cells, the basal level of SEMA3B and its responsiveness to 1,25-$(OH)_2D_3$ varied among the different lines examined (Fig. 2). It is possible that each osteoblastic cell line represents a distinct stage of osteoblast cell differentiation. Indeed, we observed a dramatic increase in SEMA3B transcript levels as MC3T3, ST-2, and primary osteoblasts differentiated into more mature osteoblasts, indicating that the process of osteoblast differentiation increases the level of native SEMA3B transcript expression. RANKL-mediated osteoclastogenesis is thought to be a primary action of early-stage osteoblasts. Thus, increased expression of SEMA3B in more differentiated, late-stage osteoblasts may not be entirely consistent with this pathway. However, the 1,25-$(OH)_2D_3$-activated expression of RANKL and SEMA3B in early-stage osteoblasts is consistent with the putative role of SEMA3B in the 1,25-$(OH)_2D_3$-stimulated, RANKL-activated osteoclastogenic pathway. Moreover, high-level expression of SEMA3B in more differentiated osteoblasts points to alternative roles for SEMA3B in other osteoblastic functions, perhaps influencing the late-stage differentiation process itself to generate mineralized matrix-producing cells. Neuropilin-1 receptors for SEMA3B are also expressed on osteoblasts (24), suggesting that SEMA3B may act in an autocrine fashion to induce osteoblast differentiation and function. This may be involved in the enhanced expression of osteoblast differentiation markers such as alkaline phosphatase in the SEMA3B-expressing transgenic osteoblasts *in vitro*. A more thorough understanding of semaphorin signaling in osteoblasts and osteoclasts is required to decipher the mechanisms through which SEMA3B stimulates osteoclast formation and bone resorption.

In summary, this study demonstrates that SEMA3B is a target gene of 1,25-$(OH)_2D_3$ in osteoblastic cells and that osteoblast-derived SEMA3B impacts skeletal homeostasis *in vivo*. This is one of the first studies to show that a member of the secreted semaphorin family exerts a biological effect on bone mineral density *in vivo* and uncovers a potential role for SEMA3B in modulating osteoclastogenesis and bone resorption.

MATERIALS AND METHODS

Cell Culture

MG-63 human osteoblastic cells were maintained in growth medium consisting of MEM supplemented with 10% fetal bovine serum (FBS), 100 U/ml penicillin, and 100 μg/ml streptomycin. MC3T3 and ST-2 cells were maintained in α-MEM (Invitrogen, Carlsbad, CA) supplemented with 10% FBS, 100 U/ml penicillin, and 100 μg/ml streptomycin. COS7 and RAW264.7 cells were maintained in DMEM containing 100 U/ml penicillin and 100 μg/ml streptomycin and 10% bovine calf serum or 10% FBS, respectively. For differentiation experiments, MC3T3, ST-2, and primary osteoblasts were grown to confluence, and then the medium was changed to growth medium supplemented with 50 μg/ml L-ascorbic acid, and 10 mM β-glycerophosphate to promote osteoblastic differentiation. Medium was replenished twice per week during the 3-wk differentiation period.

RNA Extraction and Northern Blot Analysis

mRNA was isolated from MG-63 cells with the FastTrack system (Invitrogen, Carlsbad, CA) according to the manufacturer's instructions. For bone RNA isolation, humeri were ground to a fine powder using a mortar and pestle over liquid nitrogen. Total RNA was extracted from the powder by homogenization in Trizol reagent (Invitrogen) according to the manufacturer's instructions. Total RNA was extracted from osteoblastic cell cultures using RNA-Bee (TELTEST, Friendswood, TX). RNA was separated on a formaldehyde/agarose

gel and transferred to a Duralon membrane (Stratagene, La Jolla, CA) by capillary action. The α^{32}P-labeled probes were synthesized using a Prime-A-Gene kit (Promega, Madison, WI) and hybridized to the blots using standard methods. The human SEMA3B probe, consisting of the entire human coding sequence, was obtained from pcDNA3-SEMA3B (provided by J. Minna, University of Texas Southwestern Medical Center). A 1-kb mouse SEMA3B probe was generated using RT-PCR of RNA obtained from murine osteoblasts, random hexamers (Invitrogen) were used for first-strand synthesis, and the two primers, 5′-GCTCTGCTTTCAAGAATTACA-3′ and 5′-GTCTTGCTGGGGCAGAT-3′, were used for PCR amplification. Autoradiograms were quantitated using scanning densitometry and normalized using either β-actin or GAPDH.

Immunohistochemical Detection of SEMA3B

An affinity-purified rabbit polyclonal antibody directed against human SEMA3B (residues T732–W749) was generated by Bio-synthesis Inc. (Lewisville, TX). This peptide sequence is 100% conserved between the human and mouse proteins. This same epitope was used to generate an anti-SEMA3B antibody in a previous study (21). Tibiae from 8-wk-old male C57BL/6J mice were fixed in 10% neutral buffered formalin overnight at room temperature, decalcified in Immunocal formic acid solution (American Mastertech Scientific, Lodi, CA) for 4 d at room temperature, embedded in paraffin, and sectioned. After blocking in goat serum, sections were incubated with affinity-purified anti-SEMA3B antibody (final concentration of 2.5 μg/ml). The rabbit IgG Vectastain ABC kit and the diaminobenzidine peroxidase substrate kit (Vector Laboratories, Burlingame, CA) were used for detection of the primary antibody according to the manufacturer's recommendations.

Animals and Transgenic Mouse Construction

All animal studies were approved by the Institutional Animal Care and Use Committee at Case Western Reserve University. Mice were housed in pathogen-free microisolator units with a 12-h light, 12-h dark cycle and given food and water *ad libitum*. The osteoblast-targeted transgene was constructed by replacing the *lacZ* cassette in the 2300*lacZ* plasmid (43) with the human SEMA3B coding sequence from pcDNA3-SEMA3B (20) to drive expression of SEMA3B from the 2.3-kb osteoblast-specific promoter of the mouse pro-α1(I) collagen gene. The Case Western Reserve University Transgenic Core Facility created transgenic mice by standard methods. Briefly, the transgene was linearized, purified, and injected into the pronuclei of fertilized C57B6/SJL hybrid oocytes. Oocytes were then transferred into the uteri of pseudopregnant females. Transgenic mice of the resulting progeny were identified by PCR amplification of tail genomic DNA using the following transgene-specific primers: 5′-GATTCAGCCG-GAGGGAAG-3′ located in the 3′ region of the SEMA3B cDNA and 5′-GGCATCTGCTCCTGCTTT-3′ located in the MP1 polyadenylation signal sequence. All transgenic animals and nontransgenic littermates used in these studies were greater than 95% C57BL/6J. All adult mice were killed by asphyxiation with CO_2.

Bone Mineral Density and Imaging Analysis

Tibiae from nontransgenic and transgenic littermates were dissected, fixed in formalin overnight, and transferred to 70% ethanol. Volumetric bone mineral density (milligrams per cubic centimeter) measurements of the tibiae were performed using an XCT Research pQCT densitometer (Stratec Medizintechnik, Pforzheim, Germany) as previously described (30, 44). Trabecular bone volume fraction and microarchitecture were evaluated on the proximal tibia 12 mm distal to the end of the growth plate using a μCT 40 (Scanco Medical, Southeastern, PA), and 100 12-μm slices of each bone were analyzed.

Mineralized Histology and Histomorphometry

Mice were injected ip with calcein (10 mg/kg) at 5 d before they were killed and with tetracycline (25 mg/kg) at 1 d before they were killed at 31 d of age (45). Tibiae were dissected, fixed in formalin overnight under a vacuum, and dehydrated sequentially in 70% ethanol and 95% ethanol to preserve the fluorescent labels. Longitudinal 5-μm sections were cut from methyl methacrylate plastic embedded blocks of frontal sections of each tibia. Sections were stained with Goldner's trichrome stain for the static measurements, and unstained sections were used to visualize the fluorescent labels and perform the dynamic measurements. Standard bone histomorphometry was performed as described (46) using Bioquant Image Analysis software (R & M Biometrics, Nashville, TN).

Primary Osteoblast Isolation and Differentiation

Individual calvaria were dissected from 1- to 3-d-old newborn mice, and the adherent tissue was removed. Primary osteoblasts were liberated from the bone by serial collagenase digestions (47). Cultures were established in α-MEM (Invitrogen) supplemented with 15% FBS and combined based on genotype. For differentiation studies, cells were seeded at a density of 50,000 cells per well of a six-well dish, grown to confluence, and then switched to differentiation medium containing β-glycerophosphate and ascorbic acid as described above. Alkaline phosphatase activity was determined by using a colorimetric kit that measures the conversion of *p*-nitrophenyl phosphate to *p*-nitrophenol according to the manufacturer's instructions (Sigma-Aldrich, St. Louis, MO). Alkaline phosphatase activity was normalized to protein concentration of the lysate as measured by the bicinchoninic acid (BCA) assay (Pierce Biotechnology, Inc., Rockford, IL). Mineralized nodules were visualized by staining fixed cells with 2% alizarin red S in 1% ethanol for 10 min and destaining in distilled water.

Osteoclast Differentiation and TRAP Staining

Primary osteoblasts were differentiated for 15 d as described above before overlaying osteoclast precursor cells. Osteoclast precursor cells were derived from the spleens of 7- to 10-wk-old female C57BL/6J mice. Spleen cells were plated overnight in phenol red-free α-MEM supplemented with 10% heat-inactivated FBS and 10 ng/ml macrophage colony-stimulating factor (R&D Systems, Inc., Minneapolis, MN). Nonadherent cells were added to the osteoblast cultures at a density of 500,000 cells/cm^2 in phenol red-free α-MEM containing 10% heat-inactivated FBS, 100 nM dexamethasone, and the indicated concentrations of 1,25-$(OH)_2D_3$. The cocultures were grown for an additional 8 d, and medium was replenished twice. Cells were stained for TRAP expression using the leukocyte acid phosphatase kit (Sigma-Aldrich) according to the manufacturer's instructions except that the tartrate concentration was increased to 50 mM as described (48). TRAP-positive cells with at least three nuclei were counted in triplicate wells.

RAW 264.7 Differentiation Assay

To prepare CM, COS7 cells were transfected overnight with pcDNA-SEMA3B (for CM-SEMA3B) or pcDNA empty vector (for CM-control) by standard calcium phosphate precipitation. Transfected cells were washed, and DMEM supple-

mented with 10% FBS was added. CM was collected 24 h later, filtered, and used in the RAW 264.7 assay. The presence of SEMA3B in CM was verified by Western blot.

Murine macrophage-like RAW 264.7 cells were cultured in DMEM with 10% FBS. RAW264.7 cells were seeded in 48-well plates at 2×10^3 cells per well and supplemented with 50% of CM-SEMA3B or CM-control CM with or without 20 ng/ml RANKL (R&D Systems). After 3 d, cells were stained for TRAP as described above, and the numbers of TRAP-positive multinucleated (at least three nuclei) cells were counted.

Acknowledgments

We thank Dr. Benoit de Crombrugghe for providing the 2300*lacZ* plasmid, Dr. John D. Minna for providing the pcDNA3-SEMA3B plasmid, Dr. Milan Uskokovic for providing 1,25-$(OH)_2D_3$, and Dr. Alex J. Brown for providing 24,25$(OH)_2D_3$. We also thank members of the laboratories of Dr. John H. Nilson and Dr. Ruth A. Keri for sharing their technical expertise and for helpful discussions. We are grateful to Ms. Renata Kadlcek and Dr. Edward Greenfield for assistance with the *in vitro* osteoclast assays. We are grateful to Ms. Patty Lott and the staff at the University of Alabama at Birmingham, Center for Metabolic Bone Disease, Histomorphometry and Molecular Analysis Core Laboratory, National Institutes of Health (NIH) Grant P30-AR46031, for performing the mineralized histology and histomorphometry. We acknowledge Ms. Meika Moore for the excellent technical assistance and animal handling.

Received July 25, 2007. Accepted March 11, 2008.

Address all correspondence and requests for reprints to: Paul N. MacDonald, Ph.D., Department of Pharmacology, Case Western Reserve University, 10900 Euclid Avenue, Cleveland, Ohio 44106. E-mail: paul.macdonald@case.edu.

This work was supported by NIH Grants R01 DK71769 and R01 DK 53980 (to P.N.M.), by an award from the Medical Scientist Training Program NIH Grant T32 GM007250 (to A.L.M.S.), and by a Pharmaceutical Manufacturers' Association (PhRMA) Foundation Pre-Doctoral Fellowship (to A.L.M.S.).

Disclosure Statement: A.L.M.S., X.Z., D.R.D., Y.P.K., B.S.K., and P.N.M. have nothing to declare.

REFERENCES

1. Jurutka PW, Whitfield GK, Hsieh JC, Thompson PD, Haussler CA, Haussler MR 2001 Molecular nature of the vitamin D receptor and its role in regulation of gene expression. Rev Endocr Metab Disord 2:203–216
2. Sutton AL, MacDonald PN 2003 Vitamin D: more than a "Bone-a-fide" Hormone. Mol Endocrinol 17:777–791
3. DeLuca HF 2004 Overview of general physiologic features and functions of vitamin D. Am J Clin Nutr 80: 1689S–1696S
4. Malloy PJ, Pike JW, Feldman D 1999 The vitamin D receptor and the syndrome of hereditary 1,25-dihydroxyvitamin D-resistant rickets. Endocr Rev 20:156–188
5. Horwood NJ, Elliott J, Martin TJ, Gillespie MT 1998 Osteotropic agents regulate the expression of osteoclast differentiation factor and osteoprotegerin in osteoblastic stromal cells. Endocrinology 139:4743–4746
6. Lacey DL, Timms E, Tan HL, Kelley MJ, Dunstan CR, Burgess T, Elliott R, Colombero A, Elliott G, Scully S, Hsu H, Sullivan J, Hawkins N, Davy E, Capparelli C, Eli A, Qian YX, Kaufman S, Sarosi I, Shalhoub V, Senaldi G, Guo J, Delaney J, Boyle WJ 1998 Osteoprotegerin ligand is a cytokine that regulates osteoclast differentiation and activation. Cell 93:165–176
7. Kong YY, Yoshida H, Sarosi I, Tan HL, Timms E, Capparelli C, Morony S, Oliveira-dos-Santos AJ, Van G, Itie A, Khoo W, Wakeham A, Dunstan CR, Lacey DL, Mak TW, Boyle WJ, Penninger JM 1999 OPGL is a key regulator of osteoclastogenesis, lymphocyte development and lymph-node organogenesis. Nature 397:315–323
8. van Driel M, Pols HA, van Leeuwen JP 2004 Osteoblast differentiation and control by vitamin D and vitamin D metabolites. Curr Pharm Des 10:2535–2555
9. van Leeuwen JP, van Driel M, van den Bemd GJ, Pols HA 2001 Vitamin D control of osteoblast function and bone extracellular matrix mineralization. Crit Rev Eukaryot Gene Expr 11:199–226
10. Shevde NK, Plum LA, Clagett-Dame M, Yamamoto H, Pike JW, DeLuca HF 2002 A potent analog of 1α,25-dihydroxyvitamin D3 selectively induces bone formation. Proc Natl Acad Sci USA 99:13487–13491
11. Peleg S, Uskokovic M, Ahene A, Vickery B, Avnur Z 2002 Cellular and molecular events associated with the bone-protecting activity of the noncalcemic vitamin D analog Ro-26-9228 in osteopenic rats. Endocrinology 143: 1625–1636
12. Prince CW, Butler WT 1987 1,25-Dihydroxyvitamin D3 regulates the biosynthesis of osteopontin, a bone-derived cell attachment protein, in clonal osteoblast-like osteosarcoma cells. Coll Relat Res 7:305–313
13. Yoon K, Buenaga R, Rodan GA 1987 Tissue specificity and developmental expression of rat osteopontin. Biochem Biophys Res Commun 148:1129–1136
14. Price PA, Baukol SA 1980 1,25-Dihydroxyvitamin D3 increases the synthesis of the vitamin K-dependent bone protein by osteosarcoma cells. J Biol Chem 255: 11660–11663
15. Tamagnone L, Comoglio PM 2004 To move or not to move? Semaphorin signalling in cell migration. EMBO Rep 5:356–361
16. Kolodkin AL, Levengood DV, Rowe EG, Tai YT, Giger RJ, Ginty DD 1997 Neuropilin is a semaphorin III receptor. Cell 90:753–762
17. He Z, Tessier-Lavigne M 1997 Neuropilin is a receptor for the axonal chemorepellent semaphorin III. Cell 90: 739–751
18. Tamagnon L, Artigiani S, Chen H, He Z, Ming GI, Song H, Chedotal A, Winberg ML, Goodman CS, Poo M, Tessier-Lavigne M, Comoglio PM 1999 Plexins are a large family of receptors for transmembrane, secreted, and GPI-anchored semaphorins in vertebrates. Cell 99:71–80
19. Winberg ML, Noordermeer JN, Tamagnone L, Comoglio PM, Spriggs MK, Tessier-Lavigne M, Goodman CS 1998 Plexin A is a neuronal semaphorin receptor that controls axon guidance. Cell 23:903–916
20. Sekido Y, Bader S, Latif F, Chen JY, Duh FM, Wei MH, Albanesi JP, Lee CC, Lerman MI, Minna JD 1996 Human semaphorins A(V) and IV reside in the 3p21.3 small cell lung cancer deletion region and demonstrate distinct expression patterns. Proc Natl Acad Sci USA 4120–4125
21. Tomizawa Y, Sekido Y, Kondo M, Gao B, Yokota J, Roche J, Drabkin H, Lerman MI, Gazdar AF, Minna JD 2001 Inhibition of lung cancer cell growth and induction of apoptosis after reexpression of 3p21.3 candidate tumor suppressor gene SEMA3B. Proc Natl Acad Sci USA 98:13954–13959
22. Tse C, Xiang RH, Bracht T, Naylor SL 2002 Human semaphorin 3B (SEMA3B) located at chromosome 3p21.3 suppresses tumor formation in an adenocarcinoma cell line. Cancer Res 62:542–546
23. Lallier TE 2004 Semaphorin profiling of periodontal fibroblasts and osteoblasts. J Dent Res 83:677–682
24. Harper J, Gerstenfeld LC, Klagsbrun M 2001 Neuropilin-1 expression in osteogenic cells: down-regulation

during differentiation of osteoblasts into osteocytes. J Cell Biochem 81:82–92
25. Holmes S, Downs AM, Fosberry A, Hayes PD, Michalovich D, Murdoch P, Moores K, Fox J, Deen K, Pettman G, Wattam T, Lewis C 2002 Sema7A is a potent monocyte stimulator. Scand J Immunol 56:270–275
26. Hall KT, Boumsell L, Schultze JL, Boussiotis VA, Dorfman DM, Cardoso AA, Bensussan A, Nadler LM, Freeman GJ 1996 Human CD100, a novel leukocyte semaphorin that promotes B-cell aggregation and differentiation. Proc Natl Acad Sci USA 93:11780–11785
27. Wang Z, Li Y, Wu X, Cheng S, Yang L, Wu Y 2005 KDR and Sema3 genes expression in bone marrow stromal cells and hematopoietic cells from leukemia patients and normal individuals. Hematology 10:307–312
28. Zhao M, Qiao M, Harris SE, Oyajobi BO, Mundy GR, Chen D 2004 Smurf1 inhibits osteoblast differentiation and bone formation *in vitro* and *in vivo*. J Biol Chem 279:12854–12859
29. Geoffroy V, Kneissel M, Fournier B, Boyde A, Matthias P 2002 High bone resorption in adult aging transgenic mice overexpressing cbfa1/runx2 in cells of the osteoblastic lineage. Mol Cell Biol 22:6222–6233
30. Babij P, Zhao W, Small C, Kharode Y, Yaworsky PJ, Bouxsein ML, Reddy PS, Bodine PV, Robinson JA, Bhat B, Marzolf J, Moran RA, Bex F 2003 High bone mass in mice expressing a mutant LRP5 gene. J Bone Miner Res 18:960–974
31. Wang TT, Tavera-Mendoza LE, Laperriere D, Libby E, MacLeod NB, Nagai Y, Bourdeau V, Konstorum A, Lallemant B, Zhang R, Mader S, White JH 2005 Large-scale *in silico* and microarray-based identification of direct 1,25-dihydroxyvitamin D3 target genes. Mol Endocrinol 19:2685–2695
32. Klagsbrun M, Eichmann A 2005 A role for axon guidance receptors and ligands in blood vessel development and tumor angiogenesis. Cytokine Growth Factor Rev 16: 535–548
33. Kumanogoh A, Kikutani H 2003 Roles of the semaphorin family in immune regulation. Adv Immunol 81:173–198
34. Behar O, Golden JA, Mashimo H, Schoen FJ, Fishman MC 1996 Semaphorin III is needed for normal patterning and growth of nerves, bones and heart. Nature 383: 525–528
35. Gomez C, Burt-Pichat B, Mallein-Gerin F, Merle B, Delmas PD, Skerry TM, Vico L, Malaval L, Chenu C 2005 Expression of semaphorin-3A and its receptors in endochondral ossification: potential role in skeletal development and innervation. Dev Dyn 234:393–403
36. Koh JM, Oh B, Lee JY, Lee JK, Kimm K, Kim GS, Park BL, Cheong HS, Shin HD, Hong JM, Kim TH, Park EK, Kim SY 2006 Association study of semaphorin 7a (sema7a) polymorphisms with bone mineral density and fracture risk in postmenopausal Korean women. J Hum Genet 51:112–117
37. Delorme G, Saltel F, Bonnelye E, Jurdic P, Machuca-Gayet I 2005 Expression and function of semaphorin 7A in bone cells. Biol Cell 97:589–597
38. Komori T, Yagi H, Nomura S, Yamaguchi A, Sasaki K, Deguchi K, Shimizu Y, Bronson RT, Gao YH, Inada M, Sato M, Okamoto R, Kitamura Y, Yoshiki S, Kishimoto T 1997 Targeted disruption of Cbfa1 results in a complete lack of bone formation owing to maturational arrest of osteoblasts. Cell 89:755–764
39. Otto F, Thornell AP, Crompton T, Denzel A, Gilmour KC, Rosewell IR, Stamp GW, Beddington RS, Mundlos S, Olsen BR, Selby PB, Owen MJ 1997 Cbfa1, a candidate gene for cleidocranial dysplasia syndrome, is essential for osteoblast differentiation and bone development. Cell 89:765–771
40. Liu BP, Strittmatter SM 2001 Semaphorin-mediated axonal guidance via Rho-related G proteins. Curr Opin Cell Biol 13:619–626
41. Lee NK, Choi YG, Baik JY, Han SY, Jeong DW, Bae YS, Kim N, Lee SY 2005 A crucial role for reactive oxygen species in RANKL-induced osteoclast differentiation. Blood 106:852–859
42. Razzouk S, Lieberherr M, Cournot G 1999 Rac-GTPase, osteoclast cytoskeleton and bone resorption. Eur J Cell Biol 78:249–255
43. Rossert J, Eberspaecher H, de Crombrugghe B 1995 Separate *cis*-acting DNA elements of the mouse pro-α1(I) collagen promoter direct expression of reporter genes to different type I collagen-producing cells in transgenic mice. J Cell Biol 129:1421–1432
44. Turgeman G, Zilberman Y, Zhou S, Kelly P, Moutsatsos IK, Kharode YP, Borella LE, Bex FJ, Komm BS, Bodine PV, Gazit D 2002 Systemically administered rhBMP-2 promotes MSC activity and reverses bone and cartilage loss in osteopenic mice. J Cell Biochem 86:461–474
45. Erlebacher A, Filvaroff EH, Ye JQ, Derynck R 1998 Osteoblastic responses to TGF-β during bone remodeling. Mol Biol Cell 9:1903–1918
46. Parfitt AM, Drezner MK, Glorieux FH, Kanis JA, Malluche H, Meunier PJ, Ott SM, Recker RR 1987 Bone histomorphometry: standardization of nomenclature, symbols, and units. Report of the ASBMR Histomorphometry Nomenclature Committee. J Bone Miner Res 2:595–610
47. Divieti P, Lanske B, Kronenberg HM, Bringhurst FR 1998 Conditionally immortalized murine osteoblasts lacking the type 1 PTH/PTHrP receptor. J Bone Miner Res 13: 1835–1845
48. Ragab AA, Lavish SA, Banks MA, Goldberg VM, Greenfield EM 1998 Osteoclast differentiation requires ascorbic acid. J Bone Miner Res 13:970–977

***Molecular Endocrinology* is published monthly by The Endocrine Society (http://www.endo-society.org), the foremost professional society serving the endocrine community.**